Available at www.sciencedirect.com
ScienceDirect
journal homepage: www.elsevier.com/locate/bbe

Original Research Article

Uterine myoelectrical activity as biomarker of successful induction with Dinoprostone: Influence of parity

Alba Diaz-Martinez [a], *Rogelio Monfort-Ortiz* [b], *Yiyao Ye-Lin* [a], *Javier Garcia-Casado* [a], *Mar Nieto-Tous* [b], *Félix Nieto-Del-Amor* [a], *Vicente Diago-Almela* [b], *Gema Prats-Boluda* [a,*]

[a] *Centro de Investigación e Innovación en Bioingeniería, Universitat Politècnica de València, Valencia 46022, Spain*
[b] *Servicio de Obstetricia, H.U.P. La Fe, Valencia 46026, Spain*

ARTICLE INFO

Article history:
Received 18 August 2022
Received in revised form
16 December 2022
Accepted 18 December 2022
Available online 4 January 2023

Keywords:
Electrohysterography
Labour Induction
Dinoprostone
Parity
Prolonged Labour
EHG-Biomarker

ABSTRACT

The prolonged latent phase of Induction of Labour (IOL) is associated with increased risks of maternal mortality and morbidity. Electrohysterography (EHG) has outperformed traditional clinical measures monitoring labour progress. Although parity is agreed to be of particular relevance to the success of IOL, no previous EHG-related studies have been found in the literature. We thus aimed to identify EHG-biomarkers to predict IOL success (active phase of labour in ≤ 24 h) and determine the influence of the myoelectrical response on the parity of this group. Statistically significant and sustained differences between the successful and failed groups were found from 150 min in amplitude and non-linear parameters, especially in Spectral Entropy and in their progression rates. In the nulliparous-parous comparison, parous women showed statistically significantly higher amplitude progression rate. These biomarkers would therefore be useful for early detection of the risk of induction failure and would help to develop more robust and generalizable IOL success-prediction systems.

1. Introduction

1.1. *General overview of induction of labour*

Induction of labour (IOL), defined as the process of artificially stimulating the uterus to start labour [1], is indicated when the outcome for the fetus, the mother, or both is expected to be better than waiting for the spontaneous start of labour and to prevent situations of risk such as prolonged labour, postpartum haemorrhage, foetal distress or traumatic birth [1,2]. Due to recent changes in the obstetric population's characteristics (higher maternal age, increased maternal weight

* Corresponding author.
E-mail addresses: adiaz@ci2b.upv.es (A. Diaz-Martinez), monfort_isaort@gva.es (R. Monfort-Ortiz), yiye@ci2b.upv.es (Y. Ye-Lin), jgarciac@ci2b.upv.es (J. Garcia-Casado), nieto_martou@gva.es (M. Nieto-Tous), feniede@ci2b.upv.es (F. Nieto-Del-Amor), diago_vicalm@gva.es (V. Diago-Almela), gprats@ci2b.upv.es (G. Prats-Boluda).
https://doi.org/10.1016/j.bbe.2022.12.004

and weight gain, larger newborn weights), there is a growing trend for intervention in current clinical management of labour, including IOL [3,4] whose prevalence is around 25 % worldwide [1] and 33 % in Europe [5].

Pharmacological agents such as prostaglandins are commonly used to ripen the cervix and stimulate uterine contractions to promote vaginal delivery before the spontaneous onset of labour [2]. The IOL process may take between 24 and 48 h, but its success is not guaranteed [6,7]. In fact, up to 33 % of induced patients do not respond to induction with prostaglandins or oxytocin [8]. Indeed, pharmacological induction is associated with longer hospital stays and more frequent complications than spontaneous onset of labour [9]. These include hypertonic and hyperdynamic uterine activity, foetal heart rate abnormalities, uterine rupture, meconium aspiration, water intoxication and cord prolapse post amniorrexis [10]. IOL also increases the risk of caesarean delivery by 20 %, with prolonged labour being one of its main causes (11.65 %) [9] and also of instrumental deliveries for both medical and elective inductions [11]. In addition, there is consistent evidence that the increased duration of the latent phase of labour results in increased maternal morbidity [9,12]. In comparison to the Active Phase of Labour (APL) in>24 h, women who achieved APL $\leq$ 24 h were found to have a 3.19 times lower risk of caesarean delivery, 3.23 times of chorioamnionitis, 2.98 times of endometriosis, 1.5 times of postpartum haemorrhage and, 1.59 and 1.68 times of Apgar<7 after one and five minutes [12]. Early identification of induction failure and intervention could reduce the maternal-foetal mortality and morbidity associated with prolonged labour due to the increased risk of postpartum haemorrhage and sepsis, foetal distress and asphyxia [9]. It is estimated that the cost of a caesarean after failed induction can reach $7,595 (1.3 times a standard caesarean section) in the USA [13]. In addition to the significant impact on maternal and neonatal health, IOL overloads delivery rooms and affects health care costs, with an annual cost of more than $2 billion in the USA [14]. The development of a robust and reliable system to aid IOL decision making would therefore be a key factor in enabling clinicians to better plan and manage deliveries, prevent maternal and foetal complications and optimise hospital resources.

1.2. *Risk factors for failed induction of labour*

Previous studies have identified numerous risk factors for failure of induction, such as prolonged labour, advanced maternal age, early gestational age, maternal obesity, comorbidities, oligohydramnios, foetal macrosomia, nulliparity, and unfavourable cervix [7,15]. The influence of parity on IOL is widely described in the literature [2,7,16–20]. Nulliparous women not only have a higher IOL rate than parous women (42.9 % versus 31.8 %) [2], but also have a 2.9 times higher risk of suffering from induction failure [17]. Almost half of IOLs in nulliparous women end up in instrumental delivery [11] and 37 % in caesarean section, being much lower in parous women (10 %) [21]. Friedman [18,19] first described differences in the progress of labour, finding slower progress in the first and second stages of labour (latent and active phase) for nulliparous than parous women [19]. Despite the fact that current obstetric management can substantially reduce the duration of the active phase of labour, labour progress in nulliparous women has been found to be slower than in parous [20]. In fact, the first Consensus Document on Obstetric Care suggests up to two hours of pushing in the case of parous women and three for nulliparous women before diagnosing labour arrest in the second stage [22]. Batinelli et al found that labour in parous women differed from nulliparous in term of the timing of the birth, perineal lacerations and the maternal and foetal outcome [7], suggesting that parity is of special relevance as a predictor of IOL success [7,15].

Another IOL risk factor is unfavourable cervix assessed by the Bishop score (BS) [15,23], which is a common method of predicting labour induction success in obstetrics. The BS summarizes various characteristics of cervical status in the form of a score based on: dilatation, effacement, station, consistency and position. Each element is scored from 0 to 3 points, the sum of which is the total BS [23]. However, this measure has been proven to be subjective and has low reproducibility [23,24]. Bastani et al. [25] found that the accuracy of the BS to predict induction success was low (area under the curve = 0.39), as was the area under the curve to predict induction success for other obstetric characteristics: 0.69 for cervical length [16,25], 0.72 for cervical dilatation [16] and 0.60 for foetal weight [26], so that no reliable models are currently available to predict the outcome of labour induction in clinical practice.

1.3. *The role of electrohysterography in obstetrics*

Uterine contractile activity tends to push the foetus downwards and is a key mechanism in labour together with the aforementioned cervical effacement. The electrophysiological state of the uterus may thus provide relevant information to determine the labour outcome. Electrohysterography (EHG) consists of the abdominal surface of recording of the uterine myoelectric activity generated by billions of myometrial cells. EHG recordings are made up of two different components: the Slow Wave and the Fast Wave. The former is supposed to generate the electrical conditions needed for cells to contract and the latter is associated with the contractile activity itself [27,28]. The Fast Wave is usually subdivided into two components: the Fast Wave Low, which has been associated with signal propagation; and the Fast Wave High, which is related to cellular excitability [28,29]. Terrien [30] has suggested the peak frequency of the Fast Wave Low ranges from 0.13 to 0.26 Hz and that of the Fast Wave High from 0.34 to 4 Hz. However, there is some controversy in the literature on the bandwidths of these components. The 0.1 to 0.2 frequency range is strongly influenced by the baseline oscillation and as cardiac activity mostly affects frequencies above 1 Hz, many studies consider 0.2–1 Hz to characterise the spectrum of EHG-Bursts [6,27,28,31]. EHG has been shown to outperform traditional clinical tocography in detecting uterine contractions or EHG-Bursts during pregnancy and delivery [27,31] and is especially useful for obese patients [4].

Some studies have revealed that the EHG amplitude rises as labour approaches due to increased recruitment of the cells involved in contraction [6,27,32,33]. At the same time,

the spectral content of the EHG signal shifts towards higher frequencies due to increased cell excitability [27,34–37]. The EHG signal also becomes more regular and organised, as suggested by the non-linear parameters [6,27,28,36,38,39] so that temporal, spectral and non-linear parameters have been widely used to characterise them. Previous studies demonstrated the ability of EHG parameters to distinguish the usual "ineffective" contractions during pregnancy from those associated with imminent labour ("effective" contractions), with promising results for predicting labour [9,40], preterm labour [37,41,42] and imminent labour in women with threatened preterm labour [41,43], achieving an accuracy of up to 99.7 % when predicting preterm labour [44]. As labor approaches activity becomes synchronous in order to ultimately expel the foetus, many researchers are focusing on the degree of coupling and synchronization of uterine contractions [29,45,46]. Since these studies require many electrodes on the abdomen, they mainly focus on scenarios less stressful to the mother, such as predicting preterm labor, and have achieved accuracies of up to 91 % [45]. Table 1 summarises some recently published studies in labour prediction with EHG: preterm vs term prediction; labor vs non-labour or imminent labour in women with threatened preterm labor. We have included the database used for the studies; the type of EHG segmentation used: Whole EHG Window Analysis (WEWA) or EHG-Burst Analysis (EBA); parameters calculated and prediction accuracy.

In contrast, few studies have been found that examine the uterine myoelectric response to labour induction drugs [6,59,60] despite their significant relevance as outlined above. Aviram et al. [59] studied the evolution of uterine activity during the first 12 h after Dinoprostone (E2 prostaglandins) administration. No significant changes in mean uterine muscle electrical activity were identified 0–2 h after the drug administration but a substantial increase was found after 2–8 h. In a similar study comparing electrohysterographic activity between successful and failed inductions [60], significant changes in the uterine activity index were found 210 min after Dinoprostone administration. In a former work we found no significant sustained changes in uterine myoelectric activity with respect to baseline activity (before drug administration) during the first 4 h of induction with Dinoprostone [6] or any significant differences in the drug response of uterine myoelectric activity between induction success and failure in this period, having defined induction success as the achievement of APL at any time [6]. This could indicate an important bias in that study, since oxytocin is usually administered in clinical practice to promote uterine contractility if a woman does not achieve APL in<24 h. We hypothesised that those women who achieved APL $\leq$ 24 h may exhibit a faster uterine myoelectric response to the drug than those who did not. On the other hand, as far as we are aware no study has been published focusing on the analysis of the parity effect on uterine myoelectrical activity during IOL.

The aim of this study was therefore to characterise and compare the uterine myoelectric response between induction success and failure in pregnant women given Dinoprostone drug during the first hours of IOL, induction success being defined as those women who achieved APL $\leq$ 24 h. In addition, we also aimed to assess the effect of parity on uterine myoelectric response to labour induction drugs, with the general purpose of identifying biomarkers for early detection of the risk of induction failure. For this, we determined the changes in uterine contractility by analysing a set of temporal, spectral and non-linear EHG characteristics during the first 5 h of IOL. Significant sustained differences with respect to baseline activity from 2 to 3 h after labour induction onset were found for successful inductions in EHG-biomarkers related to the number of uterine cells recruited, excitability and predictability of uterine contractions, with no significant changes for failed inductions. Successful inductions also exhibited a significantly higher progression rate (steeper slope) of these biomarkers during IOL than failed cases. As for the influence of parity, parous women with successful IOL resulted in a significantly higher progression rate of EHG signal amplitude.

2. Materials and methods

2.1. *Study design*

A prospective observational cohort study was conducted on pregnant women admitted for cervical ripening by Dinoprostone (10 mg, Propess, Ferring SAU) inserted into the posterior vaginal fornix with removal after at least 12 h in the University and Polytechnic Hospital La Fe (Valencia, Spain). Foetal macrosomia, multiple pregnancies, advanced maternal age (>45 years), severe preeclampsia, placenta praevia, premature rupture of membranes, vaginal bleeding during pregnancy, suspected foetal compromise (growth restriction, oligohydramnios, known foetal anomalies, etc.) and active cardiac, renal, pulmonary or hepatic disease; were factors for exclusion from this study due to their bias. This work adhered to the guidelines of the Declaration of Helsinki and was approved by the hospital's Institutional Review Board (Register Number 2018/0530). Patients were informed of the nature of the study and gave their written informed consent. Women who achieved APL before 24 h were included in the successful induction group (GS) and the remainder in the failed induction group (GF). The possible difference between nulliparous and parous women was analysed in the successful induction group. Since the failed induction group did not show notable uterine myoelectric activity response to the drug during the early hours of induction, as reported in the literature [6], this comparison was not included. EHG recordings began 30 min before drug administration and lasted until approximately 300 min afterwards.

The clinical data collected during the study included: maternal age, Body Mass Index (BMI), number of previous gestations, parity, gestational age at delivery, initial BS, increment of BS during IOL (12 h after insertion), achievement of APL, time to achieve APL, time to delivery, vaginal delivery ending, requirement for oxytocin, arterial newborn pH, venous newborn pH and foetal newborn weight. The chi-square test was used to detect statistically significant differences in nominal variables between the groups. Ordinal variables were compared using the Wilcoxon rank-sum test. Continuous variables were compared with the Student's *t*-

Table 1 – Selected recently published articles labour prediction with EHG. Sc: Scenario. CrD: contractions detection. BPL: biomarkers of preterm labour. PrPL: prediction of preterm labour. ImPL: imminent labour in women with threatened preterm labor. BL: biomarkers of labour. PDB: Private Database. BW: bandwidth. WEWA: Whole EHG Window Analysis. EBA: EHG-Burst Analysis. Acc: Accuracy. NA: Not available.

Sc	Author (year)	Database	Length (min)	BW (Hz)	Analysis window	Acc (%)	Significant parameters
PrPL	Fergus (2013) [47]	300 recordings (TPEHG)	30	0.34–1	WEWA	90.8	Root Mean Square, Median and Peak Frequency, Sample Entropy
PrPL	Idowu (2014) [48]	300 recordings (TPEHG)	30	0.34–1	WEWA	92.4	Root Mean Square, Median and Peak Frequency, Sample Entropy
BPL	Horoba (2016) [37]	300 recordings (TPEHG)	30	0.08–4, 0.3–4,0.3–3	WEWA	NA	Area, Auto-Correlation, Power, Max. Frequency, Median and Mean Frequency, Sample Entropy, Corr. Dim.
BPL	Lemancewicz (2016) [38]	60 recordings (PDB)	30–45	0.24–4	EBA	NA	Approximate Entropy, Binary Lempel-Ziv
BPL PrPL	Sadi-Ahmed (2017) [49]	30 recordings (TPEHG)	30	0.08–4	WEWA	95.7	Huang-Hilbert Transform, Intrinsic Mode Functions
CrD	Muszynski (2018) [50]	51 recordings (ICLEHG)	30–60	0.1–0.34	EBA	96.0	H^2 Coefficient
BPL PrPL	Mischi (2018) [41]	58 recordings (PDB)	30	0.3–0.8	EBA	73.0	Sample and Approximate Entropy
PrPL	Asmi (2018) [39]	300 recordings (TPEHG)	30	0.34–3	WEWA	95.8	Higuchi Fractal Dimension, Detrended Fluctuation Analysis
BPL PrPL	Jager (2018) [51]	326 recordings (TPEHGT, TPEHG)	30	0.08–1, 1–2.2, 2.2–3.5, 3.5–5	WEWA	100.0	Sample Entropy, Median frequency, Peak Amplitude
CrD	Hao (2019) [33]	34 recordings (PDB)	30	0–3	EBA	81.0	Power, Sample Entropy
BL	Chen (2019) [42]	122 recordings (ICLEHG)	8–86	0.1–3	EBA	90.0	Sample Entropy, Wavelet Coefficients
PrPL	You (2019) [52]	254 recordings (TPEHG)	30	0.08–4, 0.3–4, 0.3–3	WEWA	94.7	Root Mean Square, Mean Normalized Frequency, Peak and Median Frequency, Approximated Entropy, Sample Entropy
BPL ImPL	Mas-Cabo (2019) [32]	88 recordings (PDB)	30–60	0.1–4	WEWA and EBA	NA	Peak-to-Peak Amplitude, Mean and Dominant Frequency, Sample and Spectral Entropy, Time Reversibility, Binary and Multistate Lempel-Ziv
CrD BL	Allahem (2020) [53]	369 recordings (TPEHG, TPEHGT and ICLEHG)	30	NA	EBA	99.5	Amplitude, Number Of Contractions
BPL PrPL	Peng (2020) [54]	300 recordings (TPEHG)	20	0.08–4	WEWA	93.0	Sample Entropy, Median and Mean Frequency, Wavelet Coefficients, Auto-Regression.
PrPL	Prats-Boluda (2021) [43]	140 recordings (PDB)	30	0.1–4	WEWA	93.4	23 temporal, spectral and non-linear EHG parameters and 6 Obstetrical variables
BPL PrPL	Saleem (2020) [45]	26 recordings (PDB)	30	0–5	EBA	91.0	Granger Causality
PrPL	Xu (2020) [55]	300 recordings (TPEHG)	30	NA	NA	75.0	Root mean Square, Peak and Median Frequencies, Sample Entropy
PrPL	Nieto-del-Amor (2021) [56]	326 recordings (TPEHG and TPEHGT)	30	0.1–4, 0.2–0.34, 0.34–4, 0.34–1	WEWA	91.6	18 temporal, spectral and non-linear EHG parameters and 5 Obstetrical variables
PrPL	Lou (2022) [57]	300 recordings (TPEHG)	30–60	0.08–4, 0.3–3, 0.3–4	EBA	75.0	Approximate and Sample Entropy
PrPL	Allahem (2022) [58]	469 EHG (ICLEHG, TPEHG, TPEHGT and OB-1) + 552 cardiotocography (CTU-CHB) recordings	30	NA	WEWA	95.7	Amplitude, Median and Mean Frequency, Gestational Age, Maternal Age, Parity
BPL ImPL	Zhang (2022) [29]	219 recordings (PDB)	30	0.34–1	WEWA	NA	Multivariate Sample and Direct Transfer Entropy, Mutual Information, Correlation Coefficient, Coherence, Direct Partial Granger Causality
BPL PrPL	Mohammadi (2022) [44]	300 records (TPEHG)	30	0.08–4	WEWA	99.7	Empirical Mode Decomposition: Root Mean Square, Sample Entropy, Teager–Kaiser Energy

test or Wilcoxon rank-sum test, according to whether or not they were considered normal by the Shapiro-Wilk test.

2.2. Recording protocol and EHG acquisition

For the EHG recording sessions, the abdominal surface was prepared by gentle exfoliation with abrasive gel (Nuprep, Weaver and Company, Aurora, CO, USA) and cleaned with isopropyl alcohol to reduce skin-electrode impedance. Four single-use Ag/AgCl electrodes (Red Dot 2660–5, 3 M, St. Paul, MN, USA) were then placed as shown in Fig. 1. Two electrodes (M1 and M2) were symmetrically positioned with respect to the median axis at a distance of 6 cm from each other. Taking into account the gestational age of the women who underwent IOL, we decided to place the electrodes midway between the pubic symphysis and the uterine fundus, near to the navel, where signals were expected to present the highest SNR [61,62]. The other two electrodes were placed on each hip to provide reference and ground biopotentials. Both monopolar signals were conditioned by a custom-made wireless recording module, providing a 2059 V/V gain in the 0.1–150 Hz bandwidth and digitalised by a 24 bit analogue-to-digital converter at 500 Hz [63].

The digitalised monopolar EHG signals were filtered between 0.1 and 4 Hz (5th order Butterworth bandpass filter of zero phase), as the spectral content of the EHG is mainly distributed in that range, and then downsampled at 20 Hz to maintain the trade-off between temporal resolution and computational cost [28,32,64]. A bipolar signal was then calculated as their difference (M2-M1) to reduce common-mode interferences and increase signal quality [27,65]. Uterine contractions were then identified by two experts [64], in which each EHG-burst was related to substantial changes in amplitude and frequency with respect to the baseline tone with durations longer than 40 s and without respiratory interference or motion artefacts [27,31,32].

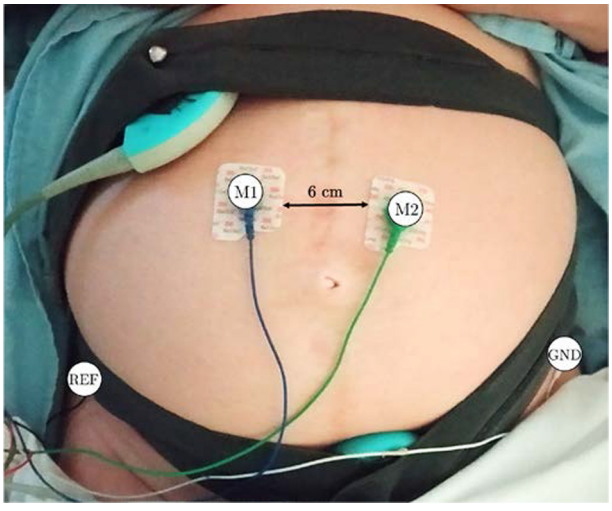

Fig. 1 – Electrodes positioning for uterine myoelectrical recording. M1: monopolar electrode 1. M2: monopolar electrode 2. REF: Reference electrode. GND: Ground electrode.

2.3. EHG parametrisation

A set of temporal, spectral, and non-linear parameters were computed to characterise uterine contractions.

2.3.1. Temporal parameters

Since obstetricians are familiar with monitoring and managing IOL, we included the following temporal parameters: Number of Contractions (NCT) and Root Mean Square (RMS), calculated in 0.1–4 Hz, as a measure of amplitude related to uterine contraction intensity [27,31–33,66].

$$RMS(x[n]) = \sqrt{\frac{1}{N}\sum_{k=1}^{N} x[n]^2} \tag{1}$$

Where x represents an EHG contraction time series and N represents its sample size. As labour progresses, the contractions are more frequent and of higher intensity, which is equivalent to a higher signal amplitude [6,27]. Both NCT and RMS are expected to show an upward trend throughout IOL.

2.3.2. Spectral parameters

As the spectral content is expected to shift towards higher frequencies due to increased cell excitability as delivery approaches, we computed the Mean Frequency (MNF) [6,37], defined as the centroid frequency of the power spectrum and is obtained as follows:

$$MNF = \frac{\sum_{k=f_L}^{f_H} PSD[k] \cdot f[k]}{\sum_{k=f_L}^{f_H} PSD[k]} \tag{2}$$

Where PSD represents the power spectral density of EHG-bursts and f the frequency distribution. The f_H and the f_L are, respectively, the upper and lower cut-off frequencies of the target bandwidth. In this work, we computed the MNF in 0.2–1 Hz to minimise the negative influence of the remainder baseline fluctuation in 0.1–0.2 Hz and the cardiac interference above 1 Hz [27,51].

We also worked out the Uterine Activity Index (UAI) [6], which provides combined information from the temporal and spectral domains. UAI was defined as the product of the peak-to-peak amplitude of the signal (App) and the $H/Lratio$ divided by duration of contractions

$$H/LRatio = \frac{\sum_{f_{L1}=0.34}^{f_{H=1}} PSD[k]}{\sum_{f_L=0.2}^{f_{H=0.34}} PSD[k]} \tag{3}$$

$$UAI = \frac{App \cdot H/LRatio}{duration} \tag{4}$$

Where PSD represents the power spectral distribution, H/L ratio is normalized energy of high frequency components (0.34–1 Hz) to low frequency ones (0.2–0.34 Hz).

2.3.3. Non-linear parameters

As labour approaches, myoelectric activity also tends to become more organised and predictable, giving rise to a downward trend in the non-linear parameters [6,56]. In this work, we also computed a set of non-linear parameters computed in the Fast Wave High bandwidth to provide robust EHG characterisation since it has been shown to better detect preterm labour and/or imminent labour [27,28]: Sample Entropy

[27,28], Spectral Entropy [6,27,64], Binary Lempel-Ziv [28,38,67] and Higuchi Fractal Dimension [39,68].

Firstly, Sample Entropy (SampEn) is a statistically measure for determining the regularity of a time series based on the existence of patterns without any previous knowledge about the source generating the dataset [69,70]. It represents the probability that similar patterns (delay vectors) in a time series will remain similar once the pattern lengths are increased (extended delay vectors), thereby providing a natural measure of the time series regularity [69,71]. Formally, given a time series x[n] of length N, a pattern vector $a_j = \{x_j, x_{j+1}, ..., x_{j+m-1}\}$ of length m is defined. $U^m(r)$ expresses the probability that the time series matches the pattern within a threshold r determined by the Chebyshev distance function $d[|x_m(j) - x_m(i)|](i \neq j)$.

$$U^m(r) = \frac{1}{N-m-1} \cdot \frac{1}{N-m} \sum_{i=1}^{N-m} \sum_{j=1, j\neq i}^{N-m} [number\ of\ times\ d[|x_m(j) - x_m(i)|] < r] \quad (5)$$

SampEn is then defined as the negative natural logarithm of the probability that two similar sequences remain similar at the next point within a tolerance, where self-comparisons are not included when calculating probability. For this work we used m = 2 and r = 0.15, as described in [6]. This parameter has been widely used both in the discrimination of preterm delivery [28,66] and also in characterising the evolution of the delivery process [6,64].

$$SampEn(m, r, N) = \begin{cases} -ln(U^{(m+1)}(r)/U^m(r)), if U^{(m+1)} \neq 0 U^m \neq 0 \\ -ln(((N-m+1))/((N-m))) \end{cases}, otherwise \quad (6)$$

Therefore, the lower value of sample entropy the more self-similarity in the time series, which is equivalent to a higher organization degree or signal regularity. The higher value of sample entropy the lower signal regularity and higher randomness of time series [69,71].

Secondly, Spectral Entropy (SpEn) is a measure of the uncertainty associated with the occurrence of a particular event at a given frequency [72]. It is computed by applying the Shannon Entropy formula to the normalised PSD of a time series x[n], such that the normalised energy of each of the frequency points is considered as a probability [73].

$$PSD_n[k] = \frac{PSD[k]^2}{\sum_{k=0}^{f_{m/2}} PSD[k]^2} \quad (7)$$

$$SpEnt = -\frac{\sum_{k=0}^{f_{m/2}} PSD_n[k] \cdot \log_2(PSD_n[k])}{\log_2(M)} \quad (8)$$

Where PSD_n[k] is the probability distribution of power spectral density of the target signal, M is the number of frequency points for which the power spectrum of the signal has been estimated and *fm* is the sampling frequency. Physically, SpEn provides information about disorder in the frequency spectrum, so that the sharper the frequency distribution, the lower the value of the parameter. Widely used to assess the progress of labour induction [6,40,64], but also in prediction of preterm labour [32]. SpEn is expected to decrease as the time of delivery approaches, suggesting a higher degree of organisation in the EHG signal spectrum.

Thirdly, the Binary Lempel-Ziv (BLZ) is a measure of the variation regularity in the time series [74,75]. The time series of the signal x[n] is firstly transformed into a finite binary sequence S (i) from left-to-right comparison with a threshold *Td*[74]. This can be expressed mathematically as:

$$S(i) = \begin{cases} 0, & if x(i) < Td \\ 1, & otherwise \end{cases} \quad (9)$$

For this we set up $Td = 0$. The resulting binary sequence is scanned sequentially looking for distinct structures or patterns, building up a dictionary that summarises the sequences seen so far [74]. Let S = {S(i)} ∀i = 1,...n denote a symbolic sequence; S(i, j) denotes a sub-sequence of S that starts at position i and ends at position j; V(S) denotes the set of all sub-sequences {S(i, j), i = 1, 2, · · · n; j ≥ i}. Starting with i = 1 and j = 1, a substring S(i, j) is compared with V(S). If S(i, j) is present in V(S), then increase j by 1 and repeat the process. Otherwise, the complexity counter c(n) is increased by one unit, since a new sub-sequence of consecutive characters is encountered, and updates i = j + 1, while the process continues until it scans the whole symbolic sequence. Physically, as labour induction progresses, uterine contractions becomes more regular, which should be reflected by lower BLZ complexity, characterized by a small number of patterns [6].

Finally, in signal analysis the fractal dimension is an index of complexity and fragmentation, comparing how the details of a signal's pattern change when measured on different scales [39,68]. It has been shown to provide relevant information in predicting preterm labour [39] and to differentiate between successful and failed labour induction [64]. In this work, we found the Higuchi fractal dimension (HFD) to be one of the most accurate and consistent fractal dimension estimation algorithms for non-periodic and irregular physiological time series signals [39,68]. Given a time series x(n), consisting of N points and a parameter $k_{max} \geq 2$, for each k∈{1, ..., k_{max}}, m∈{1, ..., k}, the length L_m(k) is defined as:

$$L_m(k) = \frac{N-1}{\frac{N-m}{k} \cdot k^2} \sum_{i=1}^{(N-m)/k} |x[m + i \cdot k] - x[m + (i-1) \cdot k]| \quad (10)$$

Then the average length L_m(k) was calculated and yielded the mean curve length L(k) for each k.

$$L(k) = \frac{\sum_{m=1}^{k} L_m(k)}{k} \quad (11)$$

HFD was thus estimated as the slope of the best linear least squares fit of the plot of ln(L(k)) versus ln(1/k) [68].

Due to the intrinsic variability of uterine contractility, we analysed the response of uterine myoelectrical activity to the induction drug in time intervals of 30 min (analysis window). We had 11 windows per record: 1 in basal condition (before drug administration) and 10 to assess the response during the first five hours of IOL. The median value of the EHG-bursts present in a 30-minute window was worked out for each plot, to obtain a single representative value per anal-

ysis window of each recording session. The mean of the parameters in the 30-minute windows was then calculated for each group, as shown in Fig. 2. To characterise the progression rate of uterine myoelectric activity throughout IOL, the slope of the median values of the 30-minute windows (a total of 11 samples) was also calculated for individual parameters and patients ($\Delta p_i/\Delta t$).

2.4. Statistical analysis

We then analysed the possible differences in uterine myoelectrical response between successful and failed (GS vs GF) inductions and identified any differences in uterine myoelectric activity between nulliparous and parous women in the induction success group during IOL (GS_N vs GS_P). To do that we first determined whether there were significant changes with respect to baseline activity for individual EHG parameters and groups (GS, GF, GS_N and GS_P) in each analysis window in the first 5 h of IOL using the Wilcoxon signed-rank test ($\alpha = 0.05$). We also determined any significant differences by means of the Wilcoxon rank sum test ($\alpha = 0.05$) for each EHG parameter and analysis window between the groups (GS vs GF and GS_N vs GS_P). Significant differences were considered to be sustained when they appeared in 4 or more consecutive 30-minute analysis windows. Finally, we worked out the Wilcoxon rank sum test ($\alpha = 0.05$) to analyse differences in the progression rates in the above-mentioned groups.

3. Results

3.1. Obstetric data and outcomes of labour induction

The 35 women who achieved APL before 24 h were included in the successful induction group (GS) and the remaining 22 in the failed induction group (GF), either because they did not reach APL or because they did so, far from the start of induction (>24 h). The possible difference between the 16 nulliparous (GS_N) and 19 parous (GS_P) women in the successful induction group was also analysed. In the GF, 16 were nulliparous and 6 were parous. Obstetric, delivery and newborn characteristics are summarised in Table 2 for both scenarios. Due to the group segregation bias, as expected, GS presented a significantly higher rate of achieving APL, shorter time to APL and delivery, reduced oxytocin augmentation and higher rate of vaginal delivery than GF. GS presented significantly lower BMI and higher progression in BS (ΔBS) than GF. No significant differences were found between the GS_N and GS_P groups except for the number of gestations and parity, which was associated with the segregation criterion.

3.2. Comparative of the success and failure of the labour induction

The evolution of uterine myoelectric activity parameters in response to the Dinoprostone labour induction drug are represented in Fig. 3 for the GS (blue) and GF (orange) groups. A steady increase in NCT was observed in the GS group throughout the recording session. Statistically significant sustained differences with respect to the baseline were found in GS from 60 min to the end. GF showed no specific trend with abrupt changes. Differences between the GS and GF groups for NCT were only found at 270 min from induction onset. As for the NCT progression rate, it did not show any significant difference between GS and GF (see violin plot Fig. 3). The RMS parameter showed a clear upward trend in GS after 60 min, suggesting increased intensity of uterine contractions, while this phenomenon was not observed in GF. Significant differences from the baseline were only found at 300 min in GS, but not in the GF group. GS showed a significantly higher amplitude than GF at 150, 180 and 270 min, with no sustained differences. Of note, GS presented a significantly higher RMS progression rate than GF in the first 5 h of induction, with a significant statistical difference, as shown by their violin plots.

In the spectral parameters, MNF presented a progressive upward trend for GS with significant sustained differences

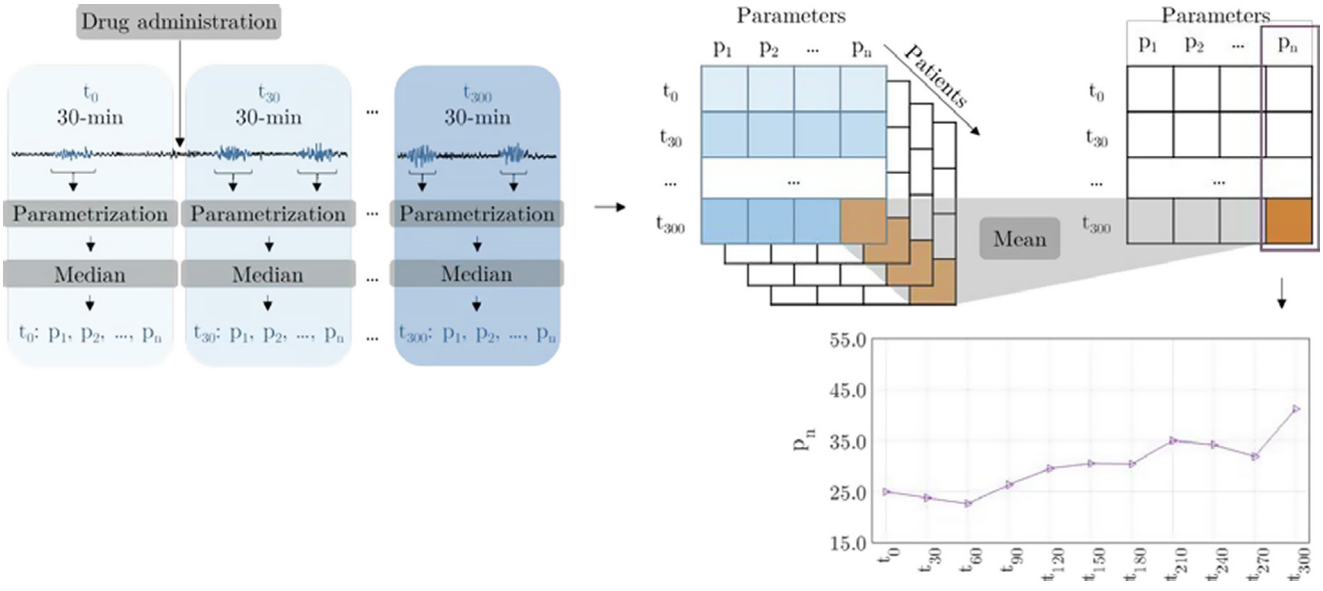

Fig. 2 – Flowchart of the parameter computation process.

Table 2 – Obstetric data and outcomes of labour induction of women enrolled in the study, mean ± standard deviation or number of cases. BMI: Body Mass Index. GAD: Gestational Age at Delivery in weeks. BS: Bishop Score. APL: Active Period of Labour. NW: Newborn Weight. p-value: Wilcoxon Rank-sum test p-value (in bold: statistically significant difference, $p < 0.05$). *: The statistical test was applied only to those achieving APL.

Variable		GS	GF	p-value	GS_N	GS_P	p-value
Maternal age (years)	$\mu\pm\sigma$	33.9 ± 5.9	34.5 ± 5.2	0.805	32.4 ± 5.4	35.3 ± 6.0	0.119
BMI (kg/m2)	$\mu\pm\sigma$	25.6 ± 6.6	27.7 ± 8.1	**0.037**	25.6 ± 8.5	25.6 ± 3.1	0.884
Gestations	$\mu\pm\sigma$	2.1 ± 1.2	1.8 ± 1.5	0.065	1.3 ± 0.5	2.8 ± 1.1	**< 0.001**
Parity	$\mu\pm\sigma$	0.7 ± 0.7	0.7 ± 0.7	0.073	0.0 ± 0.0	1.3 ± 0.5	**< 0.001**
GAD (weeks)	$\mu\pm\sigma$	40.6 ± 0.6	40.5 ± 0.7	0.801	40.6 ± 0.6	40.5 ± 0.5	0.224
Initial BS	$\mu\pm\sigma$	3.5 ± 1.7	2.9 ± 1.3	0.329	3.6 ± 1.8	3.3 ± 1.5	0.795
ΔBS	$\mu\pm\sigma$	3.9 ± 2.6	2.0 ± 1.5	**0.021**	3.1 ± 2.1	4.6 ± 2.9	0.237
Achieve APL	N	35/35	15/22	**0.002**	16/16	19/19	–
*Time to APL (h)**	$\mu\pm\sigma$	11.7 ± 5.8	28.0 ± 3.2	**< 0.001**	12.8 ± 6.3	10.7 ± 5.4	0.417
Vaginal ending	N	33/35	12/22	**0.001**	14/16	19/19	0.397
*Time to Del. (h)**	$\mu\pm\sigma$	14.7 ± 7.7	32.1 ± 10.0	**< 0.001**	17.4 ± 8.7	12.4 ± 6.0	0.085
Oxytocin	N	0/35	16/22	**< 0.001**	0/16	0/19	–
Arterial pH	$\mu\pm\sigma$	6.8 ± 1.7	6.6 ± 2.1	0.653	6.8 ± 1.8	6.9 ± 1.7	1.000
Venial pH	$\mu\pm\sigma$	7.1 ± 1.2	7.3 ± 0.1	0.420	7.3 ± 0.1	6.9 ± 1.7	0.344
NW (kg)	$\mu\pm\sigma$	3.5 ± 0.4	3.4 ± 0.3	0.166	3.5 ± 0.4	3.5 ± 0.4	0.882

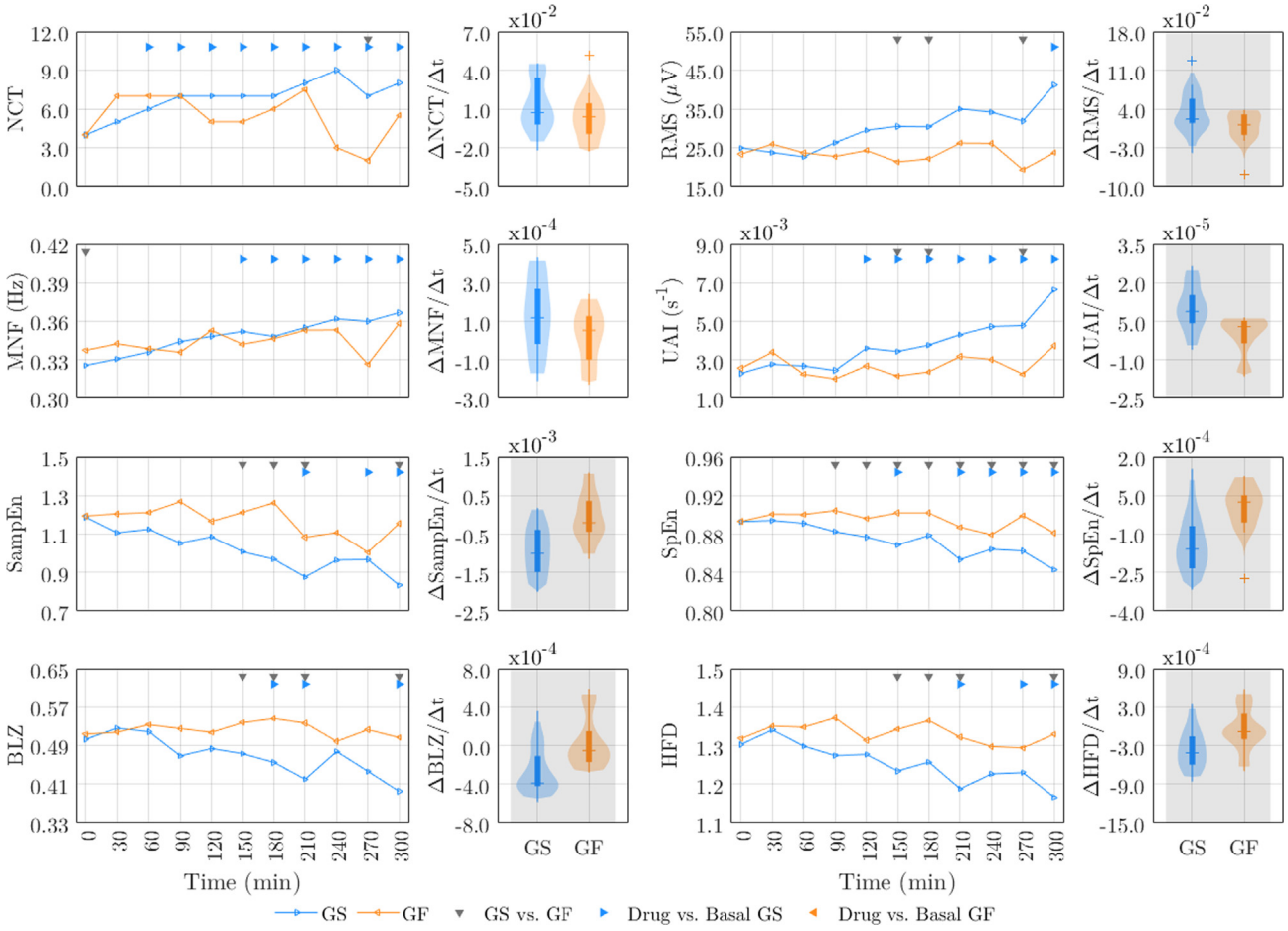

Fig. 3 – Temporal evolution of temporal, spectral and non-linear parameters and violin plots of their slopes for success (GS) and failure (GF) groups. Statistical differences between groups are indicated by grey downward-pointing triangles and with respect to basal activity by blue rightward (GS) and orange leftward (GF) triangles. In the violin plots statistical differences between GS and GF slopes are indicated by grey shading.

with respect to basal activity from 150 min until the end of the recording. Despite showing a similar trend to that of GS, the GF group did not show any statistical difference from the baseline, which may be due to the wide variability of this parameter in the GF group. Differences were only found between GF and GS at baseline. On the other hand, UAI resulted in a remarkable upward trend with significant sustained differences from baseline in GS from 120 min, which were not observed in GF. We also found significant differences between GS and GF for UAI at 150, 180 and 270 min. Even though the MNF also showed slightly higher slope values for GS, the between-group slope difference (GF vs GS) was only found for UAI as depicted in the corresponding violin plot.

Finally, as expected, non-linear parameters showed a decreasing trend in the GS group as IOL progressed. In comparison to baseline activity, the GS group obtained significant differences at some time intervals from the third hour after induction onset, without being sustained over time, for SampEn, BLZ and HFD. However, SpEn resulted in statistically significant sustained differences from 210 to the end of the recording. Again, no significant difference was found with respect to basal activity in the GF group. Significant differences between GS and GF were obtained at 150–210 and 300 for SampEn, BLZ and HFD. SpEn showed significant sustained differences between the GS and GF groups from 90 to 300 min. It is noteworthy that all non-linear parameters revealed a significantly more negative progression rate for GS than GF, with slopes statistically different.

3.3. *Comparative of nuliparous and parous uterine myoelectrical activity in labour induction success*

Fig. 4 shows the median values of the EHG parameters throughout the recording session calculated for both GS_N and GS_P, together with the violin plots of their slope distributions. GS_N showed a more pronounced increasing NCT trend throughout the recording session than GS_P, obtaining a significant difference with respect to baseline activity at some time intervals, which was not reached in GS_P group. Statistically significant differences between GS_N and GS_P were only found at 60, 270 and 300 min time intervals. As for RMS, parous women showed higher amplitude than nulliparous ones, with no significant differences between them, although GS_P had a significantly higher progression rate than GS_N.

Again, GS_N exhibited a more marked upward trend for MNF and UAI than GS_P, with significant sustained differences

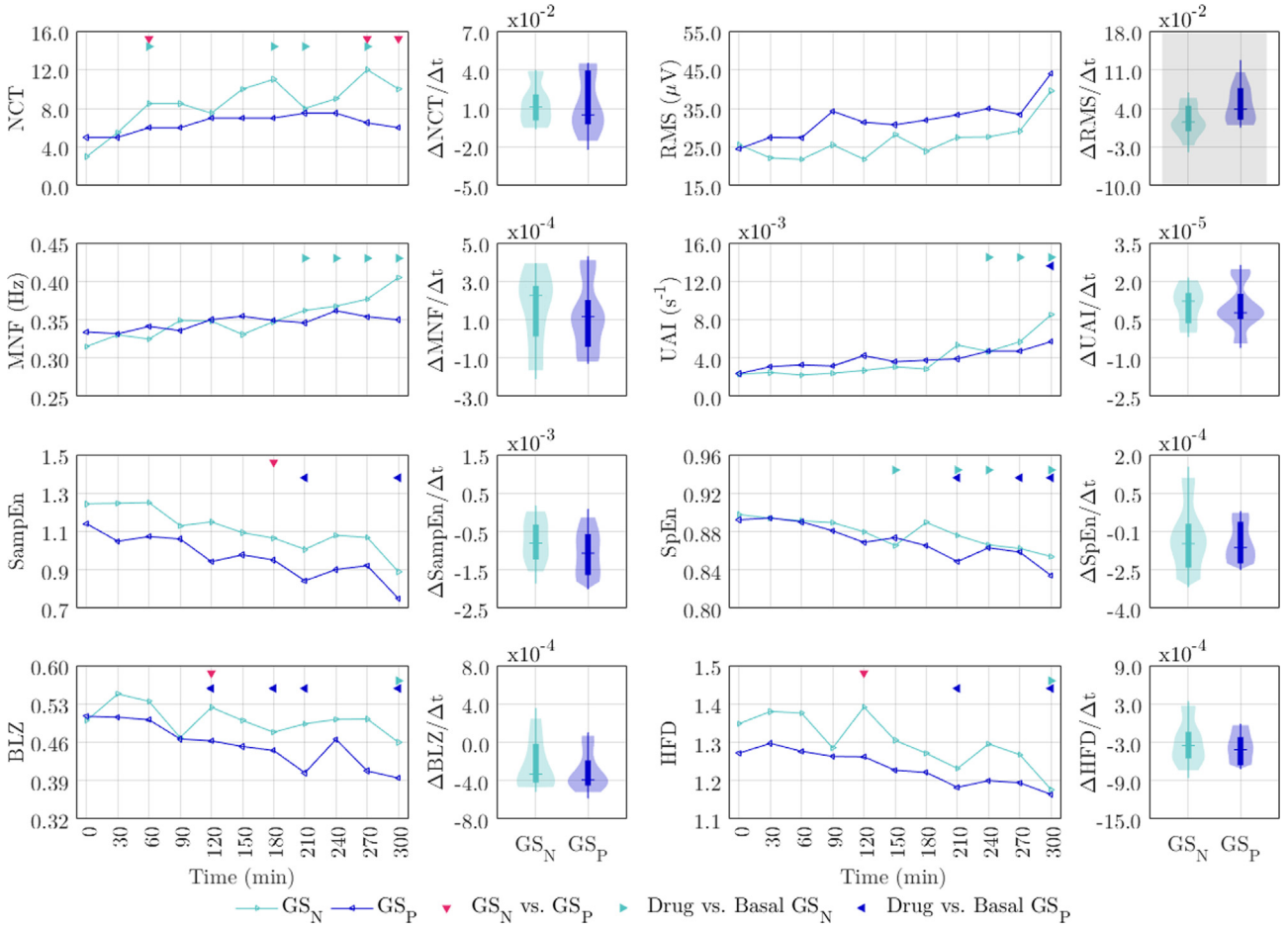

Fig. 4 – Temporal evolution of temporal, spectral and non-linear parameters and violin plots of their slopes for the Nulliparous (GS_N) and Parous Group of Success (GS_P). Statistical differences between groups are indicated by inverted pink triangles and with respect to basal activity by blue rightward (GS_N) and black leftward (GS_P) triangles. In the violin plots, statistical differences between GS_N and GS_P slopes are indicated by grey shading.

with respect to baseline activity from 210 and 240 m, respectively, for GS_N, but not for the GS_P group. We found no significant difference for either MNF or UAI or in their slopes between nulliparous and parous women.

Both GS_N and GS_P presented a similar downward tendency for non-linear parameters as labour induction progressed, GS_P achieved significant differences to baseline at some time intervals from the third hour in the four non-linear parameters, although this was not sustained over time. In contrast, GS_N reached significant SpEn differences to basal in most windows after 150 min, but this was not sustained over time. Differences were achieved for BLZ and HFD at 300 min. GS_P seemed to present a more negative progression rate for non-linear parameters than GS_N throughout the recording session, but without significant differences.

4. Discussion

4.1. *Labour induction success vs failure*

In this work we analysed and compared the difference in myoelectric uterine response to the Dinoprostone induction drug between women who achieved APL in<24 h from IOL onset (GS) and the remainder (GF). Firstly, as labour induction progressed, the uterine myoelectric activity of the GS showed an increasing trend in temporal and spectral parameters, suggesting a higher number of cells involved in contraction and also greater cell excitability [6]. This result is consistent with the fact that the increased concentration of prostaglandins E2 may induce increased myometrial contractility, this phenomenon being the indirect response of cervical ripening rather than a direct effect on the myometrium [8]. We also found that the set non-linear parameters worked out showed a downward trend for the GS group, suggesting an increased degree of organisation and predictability of the EHG signal. These findings agree with our previous studies [6,64].

We also found significant sustained changes from baseline in NCT after 60 min for spectral parameters from between 120 and 150 min and after 210 min for SpEn in the GS group. Our results are consistent with other findings in the literature that stated that changes from EHG basal activity were achieved between 2 and 8 h after administration of Dinoprostone [59] and were especially marked around the fifth hour [7,76]. Our results also agree with the pharmacokinetics of Dinoprostone: in [77] it was reported that the peak plasma level and the median time to obtain sustained uterine activity was at 60–120 and 127 min respectively after administration of vaginal Dinoprostone insert [77].

We did not obtain any significant change in uterine myoelectric activity in the GF group in comparison to baseline activity. During the first hours of IOL onset, these patients' lack of response to the drug could be related to their expression of prostaglandin receptors EP1, EP3 and EP4 in the cervix tissue, which has been shown to play an important role in delivery [8]. Konopka et al. showed that upregulated EP1 mRNA expression was associated with induction failure [78]. The increased expression of contractile EP3 and reduced expression of relaxatory EP4 in the GF group has also been reported [79]. The faster response of uterine myoelectric activity in GS is consistent with the shorter time to achieve APL, shorter time to delivery and lower percentage of women requiring oxytocin augmentation from obstetric data, which is in agreement with other findings in the literature [12,26]. It should be noted that there is some controversy over the influence of the BMI on labour induction outcomes. Batinelli [7] and Pitarello [16] found it irrelevant, while Prado et al. suggested that a lower BMI indicated a higher probability of vaginal delivery [26]. In the present work, we found that the GF group had a significantly higher BMI than GS. Since our database was relatively small, future studies will be needed to corroborate this result.

We also found significant differences between induction success and failure, especially for non-linear parameters, which we had not found in a previous study in which we only analysed the first four hours after induction onset [6]. This discrepancy could be mainly due to the definition of the induction success group, which is somewhat controversial [15]. It has been defined as achieving vaginal delivery within 24 h [12,20] or 48 h [80] after the start of labour induction [20] to any time after the start of labour induction [7]. In the present work, we opted for time-to-APL $\leq$ 24 h to avoid the bias due to oxytocin administration further promoting uterine contractility in women who do not achieve APL in 24 h. Achieving APL after 24 h may be related to the increased cell excitability associated with using of exogenous oxytocin, which is not attributable to the response to Dinoprostone.

Finally, the GS group presented a significantly higher slope than GF in almost all the EHG parameters, suggesting that the progression rate of uterine contractility contains relevant information to determine labour induction success. As the progression rate involves analysing repeated measures from different time intervals, this is undoubtedly a more reliable measure than a single measure from a specific time interval, due to intrinsic uterine contractility variability. To our knowledge, this is the first time this type of EHG-biomarker has been reported and it could be helpful in designing robust and generalizable labour induction success prediction systems.

4.2. *Influence of parity on uterine myoelectric response during IOL*

The parity effect on the IOL outcome has been extensively studied in the literature [7,16,17,22]. In general, nulliparous women seem to be less responsive than parous to Dinoprostone: a greater need for oxytocin and longer time to achieve both APL and vaginal delivery [20]. In fact, according to Batinelli et al [7], the trend changes in the Kaplan-Meier curves from the fifth hour onwards are mainly caused by the parous population, as nulliparous show this change from the eighth hour onwards [76]. Moreover, Juhasova [81] found faster cervical dilatation rates in parous than nulliparous, which could be associated with the fact that dilatation in nulliparous is pre-

ceded by a thinning of the cervix, whereas in parous both occur simultaneously [17]. In addition, nulliparous are associated with a higher risk of IOL failure [7,17], which the literature suggests could be influenced by cervical stiffness [17]. Our results on obstetric data and outcomes of labour induction are in agreement with this, although no significant differences were found. In fact, only 50 % of the nulliparous women included in the present study achieved APL $\leq$ 24 h compared to 83 % of the parous women.

In this work we specifically focused on the analysis of the effect of parity on the response of uterine myoelectric activity to the induction drug reaching APL $\leq$ 24 h, which has been little studied to date. We found a significantly higher number of contractions in nulliparous than in parous women after 4 h, which is consistent with other authors who reported that NCT was significantly lower in women with a previous delivery [82]. By contrast, we also found that parous women presented a greater uterine contraction amplitude than nulliparous women, with no significant differences at a specific time interval. This finding is consistent with the literature, given that a previous pregnancy may induce a greater number of gap-junctions in the myometrium [83]. Likewise, we found a significantly higher rate of amplitude progression in parous women, which may suggest that parous women have a greater response to prostaglandin E2. Our results partially support Ryan's findings, which reported that nulliparous have a lower uterine contractility response to oxytocin than parous women in an in vitro setting [84], as both prostaglandin E2 and oxytocin are induction drugs that promote uterine contractility. Our results of greater contraction amplitude in parous women, although with no significant differences between both groups, are consistent with [82]. In that work, it was found that women with more than one previous delivery showed a higher mean contractile force than nulliparous ones, which has been proven to be related to contraction amplitude [85]. Physiologically, vaginal parity has been linked to reduced collagen alignment and poorer biomechanical properties without affecting the overall histomorphology of the tissue [86], which may be related to the faster cervical dilatation rates in parous women [3]. Therefore, the combined interaction between uterine contractility and cervical dilatation may explain why the uterus of parous women appears to require significantly less effort to complete vaginal delivery than that of nulliparous women.

On the other hand, Prevost found that higher parity was related to lower endogen oxytocin generation and consequently to lower cell excitability [87]. This agrees with our MNF results, which are associated with cell excitability [29]. We found that the GSP group (with no grand parous women) exhibited slightly lower values and progression rates than the GSN group, with no significant difference. The non-linear parameters of the EHG showed no statistically significant differences between nulliparous and parous except for some isolated time interval and none between them. Despite of that the physiological interpretation of non-linear parameters is still unclear, we speculate that the slightly lower signal complexity in parous women may be linked with the increased coupling or synchronization degree between cells. As labor approaches, the increase of both number and density of gap junctions [88,89] gives rise to an enhanced signal propagability and higher synchronization degree at myometrium level. Indeed, using magnetomyometriogram it has been shown that parous women exhibited higher synchronization degree than nulliparous women from 36 weeks of gestation onwards [90]. Since EHG is the result of weighted sum of uterine myoelectric activity around the electrodes, an enhanced propagability is reflected as an increased signal amplitude of parous women (Fig. 4) [36]. Our hypothesis is that the more synchronized and propagated the action potentials (high connectivity between myometrium cells) the more reduced pattern number in EHG signals, which is equivalent to a more organized signal [91].

To sum up, the main differences between nulliparous and parous women consist of structural changes in the cervix, which have been associated with a higher rate of cervical dilatation in parous women. At the myometrium level, we found a lower number of contractions but faster evolution (greater progression rate) of the amplitude of the signal in parous women, but no significant differences in cell excitability or signal predictability and complexity. It is therefore important to take these factors into account when designing an induction success prediction system.

4.3. *Limitations of the study*

Despite obtaining consistent results, the present study has some limitations. Firstly, the size of the database could lead to some bias in the analysis due to intrinsic biological variability. Future work will aim to increase the sample size to corroborate the present results and to design robust and generalizable induction success prediction systems based on EHG and obstetric data.

Secondly, two approaches are commonly used in EHG signal analysis, [27]: whole EHG window analysis [28,29,44] and EHG-burst analysis [45,53,57]. The former facilitates segmenting the process, since it only requires the removal of motion artefacts from the EHG records and does not involve discrimination between uterine contraction and baseline activity [64]. Our previous study found that EHG-burst analysis to be more suitable for characterising the uterine myoelectric response to the induction drug than whole EHG-window analysis [64], while in this work the manual segmentation of contractions performed by experts in a double-blind process to reduce bias is inherently subjective and cumbersome for large datasets. Multiple systems for the automatic detection of contractions in EHG recordings during routine pregnancy monitoring [31,50] and/or threatened preterm labour [31,53] can be found in recent studies. The performance of this system in the labour induction has yet to be tested, as there may be a higher rate of movement artefacts due to maternal and foetal stress associated with imminent labour [92,93]. Also, the EHG-bursts associated with contraction can exhibit subtle changes in the latent phase of labour, making it really challenging to detect uterine contractions in this scenario.

Thirdly, we here characterised the EHG signal by assessing the degree of cell recruitment and excitability as well as uterine contraction complexity and regularity. Other indicators have been proposed based on the synchronization degree of multichannel EHG recordings to determine the uterine the degree of coupling of the uterine cell which is directly related

to the formation of the gap junction union, e.g.: iCOH [35,36], non-linear H2 [35,50], NPCMI [35,46], partial Granger causality [29,45] and partial transfer entropy [29]. Despite of the physiological interpretation of the synchronization measures, which could provide complementary information to temporal, spectral and non-linear measures, in this work we preferred to use a simplified protocol considering the highly stressful situation of labour induced for women and clinicians in clinical practice [93]. Also, a simplified protocol that does not radically alter routine clinical praxis will facilitate transferring the EHG technique to clinics. However, future work on additional simultaneous EHG recording electrodes will address the problem of obtaining additional information on the degree of synchronisation to predict successful labour induction. Despite these limitations, our findings pave the way to investigating any differences in uterine myoelectric response to other drugs, which will help to optimise drug doses and administration routes.

5. Conclusions

In this work, we analysed the different uterine myoelectric responses to Dinoprostone between labour induction success (APL $\leq$ 24 h) and failure groups (the remainder). We found significant sustained differences in EHG biomarkers with respect to baseline activity from 2 to 3 h after the start of labour induction in the successful induction group: increased number of contractions and Mean Frequency (associated with cell excitability) and reduction of SampEn and SpEn (associated with reduced complexity). In contrast, no significant changes from baseline activity were found for failed induction group. Women with successful inductions also showed a statistically higher rate of progression (steeper slope) of amplitude of the EHG-bursts and the spectral UAI parameter, and statistically lower slopes for the whole set of non-linear parameters.

We also determined the influence of parity on uterine myoelectric response to a labour induction drug in those women who achieved APL $\leq$ 24 h. Nulliparous women showed a higher number of contractions and larger changes in the mean frequency progression rate than parous women, with no significant differences between them. No differences were found in the non-linear parameters between nulliparous and parous women. The most relevant finding at the myometrium level consisted of a significantly higher progression rate of the EHG signal amplitude in parous women.

The present study not only expanded current information on electrophysiological knowledge of the in-vivo response of uterine myoelectric activity to the induction drug without the confounding factor of exogenous oxytocin, but also identified new EHG-biomarkers that could allow the early detection of the risk of induction failure. We therefore propose that they should be used to develop robust and generalizable induction success prediction systems to help clinicians to optimise induction decision-making, to better plan and manage deliveries, to prevent maternal and foetal complications and their associated mortality and morbidity and optimise hospital resources.

Funding

This work was supported by the Spanish Ministry of Economy and Competitiveness and the European Regional Development Fund (MCIU/AEI/FEDER, UE RTI2018-094449-A-I00-AR and PID2021-124038OB-I00).

Authors statement

This work adhered to the guidelines of the Declaration of Helsinki and was approved by the hospital's Institutional Review Board (Register Number 2018/0530). Patients were informed of the nature of the study and gave their written informed consent.

Declaration of Competing Interest

The authors declare that they have no known competing financial interests or personal relationships that could have appeared to influence the work reported in this paper.

Acknowledgements

Funding for open access charge: CRUE-Universitat Politècnica de València.

REFERENCES

[1] World Health Organization. WHO recommendations: Induction of labour at or beyond term. Geneva: 2018.
[2] Middleton P, Shepherd E, Crowther CA. Induction of labour for improving birth outcomes for women at or beyond term. Cochrane Database Syst Rev 2018;5:1–114. https://doi.org/10.1002/14651858.CD004945.pub4.
[3] Ashwal E, Livne MY, Benichou JIC, Unger R, Hiersch L, Aviram A, et al. Contemporary patterns of labor in nulliparous and multiparous women. American Journal of Obstetrics and Gynecology 2020;222:267.E1-267.E9. https://doi.org/10.1016/j.ajog.2019.09.035.
[4] Krogh LQ, Boie S, Henriksen TB, Thornton J, Fuglsang J, Glavind J. Induction of labour at 39 weeks versus expectant management in low-risk obese women: study protocol for a randomised controlled study. BMJ Open 2022;12:e057688.
[5] Cans C, Colver A, Krägeloh-Mann I, Platt M-J, de la Cruz J, Curran R, et al. European perinatal health report. Health and care of pregnant women and babies in Europe in 2010. 2013.
[6] Benalcazar-Parra C, Ye-Lin Y, Garcia-Casado J, Monfort-Orti R, Alberola-Rubio J, Perales A, et al. Electrohysterographic characterization of the uterine myoelectrical response to labor induction drugs. Med Eng Phys 2018;56:27–35. https://doi.org/10.1016/j.medengphy.2018.04.002.
[7] Batinelli L, Serafini A, Nante N, Petraglia F, Severi FM, Messina G. Induction of labour: clinical predictive factors for success and failure. J Obstet Gynaecol 2018;38:352–8. https://doi.org/10.1080/01443615.2017.1361388.
[8] Bakker R, Pierce S, Myers D. The role of prostaglandins E1 and E2, dinoprostone, and misoprostol in cervical ripening and the induction of labor: a mechanistic approach. Arch Gynecol

Obstet2 2017;296:167–79. https://doi.org/10.1007/s00404-017-4418-5.
[9] Vasist SN, Bhat P, Ulman S, Hebbar H. Identification of contractions from Electrohysterography for prediction of prolonged labor. J Electric Bioimpedance 2022;13:4–9. https://doi.org/10.2478/JOEB-2022-0002.
[10] Wagura P, Wasunna A, Laving A, Wamalwa D, Ng'ang'a P. Prevalence and factors associated with preterm birth at kenyatta national hospital. BMC Pregnancy and Childbirth 2018;18:107. https://doi.org/10.1186/s12884-018-1740-2.
[11] Verhoeven CJM, Oudenaarden A, Hermus MAA, Porath MM, Oei SG, Mol BWJ. Validation of models that predict Cesarean section after induction of labor. Ultrasound Obstet Gynecol 2009;34:316–21. https://doi.org/10.1002/uog.7315.
[12] Triebwasser JE, Vanartsdalen J, Kobernik EK, Seiler K, Langen ES. Assessing maternal and fetal risks associated with prolonged induction of labor. Am J Perinatol 2019;36:455–9. https://doi.org/10.1055/S-0038-1675642/ID/JR180255-14.
[13] Nicholson G, Cyr PL. Cost of failed labor induction: a Us hospital perspective. Value Health 2013;16:A75. https://doi.org/10.1016/J.JVAL.2013.03.339.
[14] Kaimal AJ, Little SE, Odibo AO, Stamilio DM, Grobman WA, Long EF, et al. Cost-effectiveness of elective induction of labor at 41 weeks in nulliparous women. Am J Obstet Gynecol 2011;204(137):e1–9. https://doi.org/10.1016/j.ajog.2010.08.012.
[15] Marconi AM. Recent advances in the induction of labor. F1000Research 2019;8:1–11. https://doi.org/10.12688/f1000research.17587.1.
[16] Pitarello P da RP, Tadashi Yoshizaki C, Ruano R, Zugaib M. Prediction of successful labor induction using transvaginal sonographic cervical measurements. Journal of Clinical Ultrasound 2012;41:76–83. https://doi.org/10.1002/jcu.21929.
[17] Delvin Anggriani D, Herawati L, Ernawati. Parity as failure determinants of labor induction in Bangka Belitung. Materia Obstetrics & Gynecology 2016;24:79–83. https://doi.org/10.20473/mog.V24I32016.79-83.
[18] Friedman EA. Primigravid labor. Obstet Gynecol 1955;6:567–89. https://doi.org/10.1097/00006250-195512000-00001.
[19] Friedman E. Labor in multiparas: a graphicostatistical analysis. Obstet Gynecol 1956;8:691–703.
[20] Kandemir O, Dede H, Yalvac S, Aldemir O, Yirci B, Yerebasmaz N, et al. The effect of parity on labor induction with prostaglandin E2 analogue (Dinoprostone): an evaluation of 2090 cases. J Preg Child Health 2015;2:1–5. https://doi.org/10.4172/2376-127X.1000149.
[21] Tan PC, Othman A, Win ST, Hong JGS, Elias N, Omar SZ. Induction of labour from 39 weeks in low-risk multiparas with ripe cervixes: a randomised controlled trial. Aust N Z J Obstet Gynaecol 2021;61:882–90. https://doi.org/10.1111/AJO.13377.
[22] Caughey AB, Cahill AG, Guise J-M, Rouse DJ. Safe prevention of the primary cesarean delivery. Am J Obstet Gynecol 2014;210:179–93. https://doi.org/10.1016/j.ajog.2014.01.026.
[23] Wormer KC, Bauer A, Williford AE. Bishop Score 2021. https://www.ncbi.nlm.nih.gov/books/NBK470368/ (accessed September 15, 2022).
[24] Kolkman DGE, Verhoeven CJM, Brinkhorst SJ, Van Der Post JAM, Pajkrt E, Opmeer BC, et al. The bishop score as a predictor of labor induction success: a systematic review. Am J Perinatol 2013;30:625–30. https://doi.org/10.1055/S-0032-1331024/ID/JR12M0145-39.
[25] Bastani P, Hamdi K, Abasalizadeh F, Pourmousa P, Ghatrehsamani F. Transvaginal ultrasonography compared with Bishop score for predicting cesarean section after induction of labor. Int J Women's Health 2011;3:277–80. https://doi.org/10.2147/IJWH.S20387.
[26] Prado CA de C, Araujo Júnior E, Duarte G, Quintana SM, Tonni G, Cavalli R de C, et al. Predicting success of labor induction in singleton term pregnancies by combining maternal and ultrasound variables. The Journal of Maternal-Fetal & Neonatal Medicine : The Official Journal of the European Association of Perinatal Medicine, the Federation of Asia and Oceania Perinatal Societies, the International Society of Perinatal Obstetricians 2016;29:3511–8. https://doi.org/10.3109/14767058.2015.1135124.
[27] Xu J, Chen Z, Lou H, Shen G, Pumir A. Review on EHG signal analysis and its application in preterm diagnosis. Biomed Signal Process Control 2022;71. https://doi.org/10.1016/J.BSPC.2021.103231 103231.
[28] Mas-Cabo J, Ye-Lin Y, Garcia-Casado J, Díaz-Martinez A, Perales-Marin A, Monfort-Ortiz R, et al. Robust characterization of the uterine myoelectrical activity in different obstetric scenarios. Entropy 2020;22:743. https://doi.org/10.3390/e22070743.
[29] Zhang Y, Hao D, Yang L, Zhou X, Ye-Lin Y, Yang Y. Assessment of Features between Multichannel Electrohysterogram for Differentiation of Labors. Sensors 2022, Vol 22, Page 3352 2022;22:3352. https://doi.org/10.3390/S22093352.
[30] Terrien J, Marque C, Gondry J, Steingrimsdottir T, Karlsson B. Uterine electromyogram database and processing function interface: An open standard analysis platform for electrohysterogram signals. Comput Biol Med 2010;40:223–30. https://doi.org/10.1016/J.COMPBIOMED.2009.11.019.
[31] Song X, Qiao X, Hao D, Yang L, Zhou X, Xu Y, et al. Automatic recognition of uterine contractions with electrohysterogram signals based on the zero-crossing rate. Sci Rep 2021;11:1–10. https://doi.org/10.1038/s41598-021-81492-1.
[32] Mas-Cabo J, Prats-Boluda G, Perales A, Garcia-Casado J, Alberola-Rubio J, Ye-Lin Y. Uterine electromyography for discrimination of labor imminence in women with threatened preterm labor under tocolytic treatment. Med Biol Eng Compu 2019;57:401–11. https://doi.org/10.1007/s11517-018-1888-y.
[33] Hao D, Qiu Q, Zhou X, An Y, Peng J, Yang L, et al. Application of decision tree in determining the importance of surface electrohysterography signal characteristics for recognizing uterine contractions. Biocybernet Biomed Eng 2019;39:806–13. https://doi.org/10.1016/J.BBE.2019.06.008.
[34] Terrien J, Marque C, Karlsson B. Spectral characterization of human EHG frequency components based on the extraction and reconstruction of the ridges in the scalogram. Ann Int Conf IEEE Eng Med Biol - Proc 2007;54:1872–5. https://doi.org/10.1109/IEMBS.2007.4352680.
[35] Mas-Cabo J, Ye-Lin Y, Garcia-Casado J, Alberola-Rubio J, Perales A, Prats-Boluda G. Uterine contractile efficiency indexes for labor prediction: a bivariate approach from multichannel electrohysterographic records. Biomed Signal Process Control 2018;46:238–48. https://doi.org/10.1016/j.bspc.2018.07.018.
[36] García-Casado J, Ye-Lin Y, Prats-Boluda G, Mas-Cabo J, Alberola-Rubio J, Perales A. Electrohysterography in the diagnosis of preterm birth: a review. Physiol Meas 2018;39:1–23. https://doi.org/10.1088/1361-6579/aaad56.
[37] Horoba K, Jezewski J, Matonia A, Wrobel J, Czabanski R, Jezewski M. Early predicting a risk of preterm labour by analysis of antepartum electrohysterograhic signals. Biocybernet Biomed Eng 2016;36:574–83. https://doi.org/10.1016/J.BBE.2016.06.004.
[38] Lemancewicz A, Borowska M, Kuć P, Jasińska E, Laudański P, Laudański T, et al. Early diagnosis of threatened premature labor by electrohysterographic recordings - the use of digital signal processing. Biocybernet Biomed Eng 2016;36:302–7. https://doi.org/10.1016/J.BBE.2015.11.005.

[39] Asmi PS, Subramaniam K, Iqbal NV. Classification of fractal features of uterine EMG signal for the prediction of preterm birth. Biomed Pharmacol J 2018;11:369–74. https://doi.org/10.13005/BPJ/1381.
[40] Benalcazar-Parra C, Ye-Lin Y, Garcia-Casado J, Monfort-Ortiz R, Alberola-Rubio J, Perales A, et al. Prediction of labor induction success from the uterine electrohysterogram. Hindawi J Sensors 2019;2019:1–12. https://doi.org/10.1155/2019/6916251.
[41] Mischi M, Chen C, Ignatenko T, De Lau H, Ding B, Guid Oei SG, et al. Dedicated entropy measures for early assessment of pregnancy progression from single-channel electrohysterography. IEEE Trans Biomed Eng 2018;65:875–84. https://doi.org/10.1109/TBME.2017.2723933.
[42] Chen L, Hao Y, Hu X. Detection of preterm birth in electrohysterogram signals based on wavelet transform and stacked sparse autoencoder. PLoS One 2019;14:e0214712.
[43] Prats-Boluda G, Pastor-Tronch J, Garcia-Casado J, Monfort-Ortíz R, Perales Marín A, Diago V, et al. Optimization of imminent labor prediction systems in women with threatened preterm labor based on electrohysterography. Sensors 2021;21:2496. https://doi.org/10.3390/S21072496.
[44] Mohammadi Far S, Beiramvand M, Shahbakhti M, Augustyniak P. Prediction of preterm delivery from unbalanced EHG database. Sensors 2022;22:1507. https://doi.org/10.3390/S22041507.
[45] Saleem S, Saeed A, Usman S, Ferzund J, Arshad J, Mirza J, et al. Granger causal analysis of electrohysterographic and tocographic recordings for classification of term vs. preterm births. Biocybernet Biomed Eng 2020;40:454–67. https://doi.org/10.1016/J.BBE.2020.01.007.
[46] Mas-Cabo J, Prats-Boluda G, Garcia-Casado J, Alberola-Rubio J, Perales A, Ye-Lin Y. Design and assessment of a robust and generalizable expert system for the prediction of premature birth by means of multi-channel electrohysterographic records. J Title: J Sensors 2019;7:1–13. https://doi.org/10.1155/2019/5373810.
[47] Fergus P, Cheung P, Hussain A, Al-Jumeily D, Dobbins C, Iram S. Prediction of preterm deliveries from EHG signals using machine learning. PLoS One 2013;8:1–16. https://doi.org/10.1371/journal.pone.0077154.
[48] Idowu IO, Fergus P, Hussain A, Dobbins C, Al-Askar H. Advance artificial neural network classification techniques using EHG for detecting preterm births. Proceedings - 2014 8th International Conference on Complex, Intelligent and Software Intensive Systems, CISIS 2014 2014:95–100. https://doi.org/10.1109/CISIS.2014.14.
[49] Sadi-Ahmed N, Kacha B, Taleb H, Kedir-Talha M. Relevant features selection for automatic prediction of preterm deliveries from pregnancy ElectroHysterograhic (EHG) records. J Med Syst 2017;41:204. https://doi.org/10.1007/S10916-017-0847-8.
[50] Muszynski C, Happillon T, Azudin K, Tylcz JB, Istrate D, Marque C. Automated electrohysterographic detection of uterine contractions for monitoring of pregnancy: feasibility and prospects. BMC Pregnancy Childbirth 2018;18:1–8. https://doi.org/10.1186/S12884-018-1778-1/TABLES/2.
[51] Jager F, Libenšek S, Geršak K. Characterization and automatic classification of preterm and term uterine records. PLoS One 2018;13:e0202125.
[52] You J, Kim Y, Seok W, Lee S, Sim D, Park KS, et al. Multivariate time-frequency analysis of electrohysterogram for classification of term and preterm labor. J Electr Eng Technol 2019;14:897–916. https://doi.org/10.1007/s42835-019-00118-9.
[53] Allahem H, Sampalli S. Automated uterine contractions pattern detection framework to monitor pregnant women with a high risk of premature labour. Inf Med Unlocked 2020;20. https://doi.org/10.1016/J.IMU.2020.100404 100404.
[54] Peng J, Hao D, Yang L, Du M, Song X, Jiang H, et al. Evaluation of electrohysterogram measured from different gestational weeks for recognizing preterm delivery: a preliminary study using random Forest. Biocybernet Biomed Eng 2020;40:352–62. https://doi.org/10.1016/J.BBE.2019.12.003.
[55] Xu J, Chen Z, Lu Y, Yang X, Pumir A. Improved Preterm Prediction Based on Optimized Synthetic Sampling of EHG Signal 2020. https://doi.org/https://doi.org/10.48550/arXiv.2007.01447.
[56] Nieto-Del-amor F, Prats-Boluda G, Martinez-De-juan JL, Diaz-Martinez A, Monfort-Ortiz R, Diago-Almela VJ, et al. Optimized feature subset selection using genetic algorithm for preterm labor prediction based on electrohysterography. Sensors 2021;21:3350. https://doi.org/10.3390/S21103350.
[57] Lou H, Liu H, Chen Z, Zhen Z, Dong B, Xu J. Bio-process inspired characterization of pregnancy evolution using entropy and its application in preterm birth detection. Biomed Signal Process Control 2022;75. https://doi.org/10.1016/J.BSPC.2022.103587 103587.
[58] Allahem H, Sampalli S. Automated labour detection framework to monitor pregnant women with a high risk of premature labour using machine learning and deep learning. Inf Med Unlocked 2022;28. https://doi.org/10.1016/J.IMU.2021.100771 100771.
[59] Aviram A, Melamed N, Hadar E, Raban O, Hiersch L, Yogev Y. Effect of prostaglandin E2 on myometrial electrical activity in women undergoing induction of labor. Am J Perinatol 2014;31:413–8. https://doi.org/10.1055/S-0033-1352486.
[60] Toth T. Transcutaneous electromyography of uterus in prediction of labor outcome induced by oxytocine and prostaglandine shapes. Gynaecol Perinatol 2005;14:75–85.
[61] Xu Y, Hao D, Taggart MJ, Zheng D. Regional identification of information flow termination of electrohysterographic signals: towards understanding human uterine electrical propagation. Comput Methods Programs Biomed 2022;223. https://doi.org/10.1016/J.CMPB.2022.106967 106967.
[62] Rabotti C, Mischi M, Van Laar JOEH, Oei GS, Bergmans JWM. Estimation of internal uterine pressure by joint amplitude and frequency analysis of electrohysterographic signals. Physiol Meas 2008;29:829–41. https://doi.org/10.1088/0967-3334/29/7/011.
[63] Ye-Lin Y, Bueno-Barrachina JM, Prats-boluda G, Rodriguez de Sanabria R, Garcia-Casado J. Wireless sensor node for non-invasive high precision electrocardiographic signal acquisition based on a multi-ring electrode. Measurement 2017;97:195–202. https://doi.org/10.1016/J.MEASUREMENT.2016.11.009.
[64] Diaz-Martinez A, Monfort-Ortiz R, Ye-Lin Y, Garcia-Casado J, Nieto-Del-Amor F, Diago-Almela VJ, et al. Comparative study of uterine myoelectrical response to labour induction drugs in nulliparous and parous women with different EHG analysis techniques. Int Conf E-Health Bioeng (EHB) 2021;2021:1–4. https://doi.org/10.1109/EHB52898.2021.9657548.
[65] Alberola-Rubio J, Prats-Boluda G, Ye-Lin Y, Valero J, Perales A, Garcia-Casado J. Comparison of non-invasive electrohysterographic recording techniques for monitoring uterine dynamics. Med Eng Phys 2013;35:1736–43. https://doi.org/10.1016/j.medengphy.2013.07.008.
[66] Xu J, Wang M, Zhang J, Chen Z, Huang W, Shen G, et al. Network theory based EHG signal analysis and its application in preterm prediction. IEEE J Biomed Health Inform 2022;26:2876–87. https://doi.org/10.1109/JBHI.2022.3140427.

[67] Talebinejad M, Chan ADC, Miri A. A Lempel-Ziv complexity measure for muscle fatigue estimation. J Electromyogr Kinesiol : Off J Int Soc Electrophysiol Kinesiol 2011;21:236–41. https://doi.org/10.1016/j.jelekin.2010.12.003.
[68] Kesić S, Spasić SZ. Application of Higuchi's fractal dimension from basic to clinical neurophysiology: a review. Comput Methods Programs Biomed 2016;133:55–70. https://doi.org/10.1016/J.CMPB.2016.05.014.
[69] Richman JS, Moorman JR. Physiological time-series analysis using approximate and sample entropy. Am J Physiol Heart Circ Physiol 2000;278:2039–49. https://doi.org/10.1152/ajpheart.2000.278.6.H2039.
[70] Fele-Žorž G, Kavšek G, Novak-Antolič Ž, Jager F. A comparison of various linear and non-linear signal processing techniques to separate uterine EMG records of term and pre-term delivery groups. Med Biol Eng Compu 2008;46:911–22. https://doi.org/10.1007/s11517-008-0350-y.
[71] Delgado-Bonal A, Marshak A. Entropy approximate entropy and sample entropy: a comprehensive tutorial. Entropy 2019;21:541. https://doi.org/10.3390/e21060541.
[72] Devi D, Sophia S, Boselin Prabhu SR. Deep learning-based cognitive state prediction analysis using brain wave signal. Cognitive Comput Hum-Robot Interact: Principles Pract 2021:69–84. https://doi.org/10.1016/B978-0-323-85769-7.00017-3.
[73] Shannon CE. A mathematical theory of communication. Bell Syst Tech J 1948;27:379–423. https://doi.org/10.1002/J.1538-7305.1948.TB01338.X.
[74] Lempel A, Ziv J. On the complexity of finite sequences. IEEE Trans Inf Theory 1976;22:75–81. https://doi.org/10.1109/TIT.1976.1055501.
[75] Aboy M, Hornero R, Abásolo D, Álvarez D. Interpretation of the Lempel-Ziv complexity measure in the context of biomedical signal analysis. IEEE Trans Biomed Eng 2006;53:2282–8. https://doi.org/10.1109/TBME.2006.883696.
[76] Rhomadona SW, Widyawati MN, Suryono S. Monitoring of uterus electrical activities using electromyography in stage I induction labor. J Phys Conf Ser 2018;1179:1–6. https://doi.org/10.1088/1742-6596/1179/1/012133.
[77] Yount SM, Lassiter N. The pharmacology of prostaglandins for induction of labor. J Midwifery Womens Health 2013;58:133–44. https://doi.org/10.1111/JMWH.12022.
[78] Konopka CK, Glanzner WG, Rigo ML, Rovani MT, Comim FV, Gonçalves PBD, et al. Responsivity to PGE2 labor induction involves concomitant differential prostaglandin E receptor gene expression in cervix and myometrium. Genet Mol Res: GMR 2015;14:10877–87. https://doi.org/10.4238/2015.SEPTEMBER.9.25.
[79] Roos N, Blesson CS, Stephansson O, Masironi B, Vladic Stjernholm Y, Ekman-Ordeberg G, et al. The expression of prostaglandin receptors EP3 and EP4 in human cervix in post-term pregnancy differs between failed and successful labor induction. Acta Obstet Gynecol Scand 2014;93:159–67. https://doi.org/10.1111/AOGS.12300.
[80] Indraccolo U, Scutiero G, Greco P. Sonographic cervical shortening after labor induction is a predictor of vaginal delivery. Revista Brasileira de Ginecologia e Obstetricia 2016;38:585–8. https://doi.org/10.1055/s-0036-1597629.
[81] Juhasova J, Kreft M, Zimmermann R, Kimmich N. Impact factors on cervical dilation rates in the first stage of labor. J Perinat Med 2018;46:59–66. https://doi.org/10.1515/jpm-2016-0284.
[82] Ryan GA, Nicholson SM, Crankshaw DJ, Morrison JJ. Maternal parity and functional contractility of human myometrium in vitro in the third trimester of pregnancy. J Perinatol 2019;39:439–44. https://doi.org/10.1038/s41372-019-0312-2.
[83] Gerli S, Favilli A, Giordano C, Bini V, Di Renzo GC. Single indications of induction of labor with prostaglandins and risk of cesarean delivery: a retrospective cohort study. J Obstet Gynaecol Res 2013;39:926–31. https://doi.org/10.1111/JOG.12000.
[84] Ryan GA, Crankshaw DJ, Morrison JJ. Effects of maternal parity on response of human myometrium to oxytocin and ergometrine in vitro. Eur J Obstet Gynecol Reprod Biol 2019;242:99–102. https://doi.org/10.1016/j.ejogrb.2019.09.006.
[85] Benalcazar-Parra C, Garcia-Casado J, Ye-Lin Y, Alberola-Rubio J, Lopez Á, Perales-Marin A, et al. New electrohysterogram-based estimators of intrauterine pressure signal, tonus and contraction peak for non-invasive labor monitoring. Physiol Meas 2019;40:1–24. https://doi.org/10.1088/1361-6579/ab37db.
[86] Feola A, Abramowitch S, Jones K, Stein S, Moalli P. Parity negatively impacts vaginal mechanical properties and collagen structure in rhesus macaques. Am J Obstet Gynecol 2010;203(595):e1–8. https://doi.org/10.1016/J.AJOG.2010.06.035.
[87] Prevost M, Zelkowitz P, Tulandi T, Hayton B, Feeley N, Carter CS, et al. Oxytocin in pregnancy and the postpartum: relations to labor and its management. Front Public Health 2014;2:1–9. https://doi.org/10.3389/FPUBH.2014.00001/BIBTEX.
[88] Garfield RE, Maner WL. Physiology and electrical activity of uterine contractions. Semin Cell Dev Biol 2007;18:289–95. https://doi.org/10.1016/j.semcdb.2007.05.004.
[89] Garfield RE, Blennerhassett MG, Miller SM. Control of myometrial contractility: role and regulation of gap junctions. Oxf Rev Reprod Biol 1988;10:436–90.
[90] Govindan RB, Siegel E, McKelvey S, Murphy P, Lowery CL, Eswaran H. Tracking the changes in synchrony of the electrophysiological activity as the uterus approaches labor using magnetomyographic technique. Reprod Sci 2015;22:595–601. https://doi.org/10.1177/1933719114556484.
[91] Mas-Cabo J, Prats-Boluda G, Ye-Lin Y, Alberola-Rubio J, Perales A, Garcia-Casado J. Characterization of the effects of Atosiban on uterine electromyograms recorded in women with threatened preterm labor. Biomed Signal Process Control 2019;52:198–205. https://doi.org/10.1016/j.bspc.2019.04.001.
[92] Ye-Lin Y, Garcia-Casado J, Prats-Boluda G, Alberola-Rubio J, Perales A. Automatic identification of motion artifacts in EHG recording for robust analysis of uterine contractions. Comput Math Methods Med 2014;2014:1–11. https://doi.org/10.1155/2014/470786.
[93] Kagwisage J, S Balandya B, B Pembe A, GM Mujinja P. Health Related Quality of Life Post Labour Induction with Misoprostol Versus Dinoprostone At Muhimbili National Hospital in Dar Es Salaam, Tanzania: A cross Sectional Study. The East African Health Research Journal 2020;4:58–64. https://doi.org/10.24248/EAHRJ.V4I1.622.